Appendix A

Numerical evaluation of periodic orbits

This technical appendix describes numerical techniques to deal with classical periodic orbits. Efficient methods for finding those orbits, calculating the relevant properties for the trace formula, and following them through parameter space are presented.

Contents

A.1 Finding periodic orbits

The numerical determination of periodic orbits in an arbitrary potential includes three steps:

1. Integration of the classical equations of motion (EOM).
2. Calculation of the variation of the endpoint for small changes of the starting point.
3. Calculating an improved starting point.

Beginning with randomly distributed starting points, these steps are iterate until convergence.

A.1.1 Integrating the equations of motion

The equations of motion are readily integrated numerically. For a sufficient performance of this innermost step in the semiclassical calculation an efficient scheme with adaptive step-size control should be implemented. For smooth potentials, the algorithm presented by Bulirsch and Stoer [104, 107] is accepted to be one of the most powerful methods available.

A.1.2 The matrizant

Calculating the effect of a small change of the starting point by integrating trajectories at small, but finite distances suffers from severe numerical limitations. The numerical roundoff gets worse for larger $|\mathrm{Tr}(\widetilde{M})|$ and is intolerable already for moderately unstable orbits. Eckhardt and Wintgen [25] presented a method which is better adapted to the limitations of a numerical approach. It will be outlined in the following.

Denoting the phase space vector of the reference trajectory with $\boldsymbol{\gamma} = (\boldsymbol{q}, \boldsymbol{p})$ with the coordinates $\boldsymbol{q}$ and the canonical conjugate momenta $\boldsymbol{p}$, the EOM can be written as

$$\dot{\boldsymbol{\gamma}} = \underline{J}\,\frac{\partial H}{\partial \gamma} \quad \text{with} \quad \underline{J} := \begin{pmatrix} 0 & \mathbb{1} \\ -\mathbb{1} & 0 \end{pmatrix} . \tag{A.1}$$

Here and in the following, the dots signify derivatives with respect to time. The linearized time evolution of the difference vector to the reference orbit $\delta\boldsymbol{\gamma}$ is given by

$$\delta\boldsymbol{\gamma}(t) \;=\; \underline{\chi}(t)\;\delta\boldsymbol{\gamma}(0)\;, \tag{A.2}$$

with the *matrizant* $\underline{\chi}$. The time evolution of $\underline{\chi}$ can be shown to be

$$\dot{\underline{\chi}} \;=\; L\cdot\underline{\chi} \quad \text{with} \quad \underline{L}(t) \;=\; \underline{J}\;\left.\frac{\partial^2 H}{\partial \boldsymbol{\gamma}^2}\right|_{\boldsymbol{\gamma}(t)} , \tag{A.3}$$

and $\underline{\chi}(0) = \mathbb{1}$. For periodic orbits, the *monodromy matrix*[1] M is defined as $M = \underline{\chi}(T)$, where T is the period of the orbit.

[1] To be consistent with the standard notation in trace formulae, the monodromy matrix is denoted without underscore.

The matrizant is symplectic, i. e. $\underline{\chi}^\dagger \underline{J}\,\underline{\chi} = \underline{J}$, and two eigenvalues of $\underline{\chi}$ are equal to 1 (see Eq. (A.5) below). One of these trivial eigenvalues is associated with energy conservation, the other with the displacement along the trajectory. The corresponding eigenvectors can be eliminated analytically. This will be sketched in the following for two dimensional systems. From now on, $\boldsymbol{\gamma} = (x, y, u, v)$.

Introducing a local coordinate system by the unitary transformation $\underline{U}(t)$ according to

$$\delta\widehat{\boldsymbol{\gamma}} \;=\; \underline{U}(t)\,\delta\boldsymbol{\gamma} \quad \text{with} \quad \underline{U}(t) \;=\; \begin{pmatrix} \dot{x} & -\dot{u}/q^2 & -\dot{y} & -\dot{v}/q^2 \\ \dot{y} & -\dot{v}/q^2 & \dot{x} & \dot{u}/q^2 \\ \dot{u} & \dot{x}/q^2 & \dot{v} & -\dot{y}/q^2 \\ \dot{v} & \dot{y}/q^2 & -\dot{u} & \dot{x}/q^2 \end{pmatrix} , \tag{A.4}$$

where $q = |\dot{\boldsymbol{\gamma}}|$ leads to a transformed matrizant

$$\delta\widehat{\boldsymbol{\gamma}}(t) \;=\; \underline{\widehat{\chi}}(t)\,\delta\widehat{\boldsymbol{\gamma}}(0) \quad \text{with} \quad \underline{\widehat{\chi}}(t) \;=\; \underline{U}^{-1}(t)\,\underline{\chi}(t)\,\underline{U}(0) \;=\; \begin{pmatrix} 1 & * & * & * \\ 0 & 1 & 0 & 0 \\ 0 & * & & \\ 0 & * & \multicolumn{2}{c}{\underline{\widetilde{\chi}}(t)} \end{pmatrix} . \tag{A.5}$$

In this coordinate system the two eigenvalues of 1 can be seen explicitly. The time evolution of the reduced matrizant $\underline{\widetilde{\chi}}(t)$ is given by

$$\dot{\underline{\widetilde{\chi}}}(t) \;=\; \underline{l}(t)\,\underline{\widetilde{\chi}}(t) \quad \text{with} \quad \underline{l} \;=\; \underline{U}^{-1}(\underline{L}\,\underline{U} - \dot{\underline{U}}) \,. \tag{A.6}$$

Denoting the partial derivatives of the Hamiltonian by subscripts, i. e. $H_x = \partial H/\partial x$, the matrix $\underline{l}$ is explicitly given by

$$\begin{aligned} \underline{l} \;&=\; \begin{pmatrix} l_{11} & l_{12} \\ l_{21} & l_{22} \end{pmatrix} , \quad \text{with} \qquad\qquad (A.7)\\ l_{11} \;&=\; \big[(-H_{xx} - H_{yy} + H_{uu} + H_{vv})(H_x H_u + H_y H_v) \\ &\quad +(-H_x^2 + H_y^2 + H_u^2 - H_v^2)(H_{yv} + H_{xu}) + 2(H_x H_y - H_u H_v)(H_{xv} + H_{yu})\big]/q^2 \\ l_{12} \;&=\; \big[(H_{xx} + H_{vv})(H_y^2 + H_u^2) + (H_{yy} + H_{uu})(H_x^2 + H_v^2) \\ &\quad -2(H_x H_u + H_y H_v)(H_{xu} + H_{yv}) - 2(H_x H_y - H_u H_v)(H_{xy} - H_{uv})\big]/q^4 \\ l_{21} \;&=\; \big[-(H_{xx} + H_{yy})(H_u^2 + H_v^2) - (H_{uu} + H_{vv})(H_x^2 + H_y^2) \\ &\quad +2(H_x H_v + H_y H_u)(H_{xv} + H_{yu}) + 2(H_x H_u - H_y H_v)(H_{xu} - H_{yv})\big] \\ l_{22} \;&=\; -l_{11} \,. \end{aligned}$$

These formulae have been derived by Eckhardt and Wintgen [25]. They shall now be applied to a particle in a homogeneous magnetic field and a velocity-independent external potential V. For this situation, it is convenient to express $\underline{l}$ in dependence of the real space coordinates and their time derivatives. This finally leads to

$$\begin{aligned} l_{11} \;&=\; \left(2 - w_c^2/2 - V_{xx} - V_{yy}\right)\left(\dot{x}V_x + \dot{y}V_y\right)/q^2 \qquad\qquad (A.8)\\ l_{12} \;&=\; \left(1 + (w_c/2)^2\right)/q^2 + \left[V_{xx}(\dot{x}^2 + \beta^2) + V_{yy}(\dot{y}^2 + \alpha^2) + 2V_{xy}(\dot{x}\dot{y} - \alpha\beta)\right]/q^4 \\ l_{21} \;&=\; -\left(V_{xx} + V_{yy} + w_c^2/2\right)\left(\dot{x}^2 + \dot{y}^2\right) - 2\left(\alpha^2 + \beta^2\right) \\ l_{22} \;&=\; -l_{11} \,. \end{aligned}$$

with $w_c = eB/m^\star$, $\alpha = (V_x - \dot{y}w_c/2)$ and $\beta = (V_y + \dot{x}w_c/2)$. Starting from the initial condition $\underline{\widetilde{\chi}}(0) = \mathbb{1}$, Eq. (A.6) can be integrated. The most effective approach is to solve the equations of motion for $\underline{\widetilde{\chi}}$ and the time evolution of the trajectory simultaneously. This leads to four equations for the phase-space motion and another four for $\underline{\widetilde{\chi}}$. Without reduction of the matrizant to two dimensions, a $(4 \times 4 + 4 =)$ 20-dimensional differential equation has to be solved. This integration is the innermost loop of the calculation, so that the analytical reduction of the monodromy matrix speeds up the the semiclassical approximation by a factor of about 2.

The matrizant gives the linearization of *arbitrary* deviations from $\boldsymbol{\gamma}(t)$. In the following section this information will be used in a numerical scheme to converge to periodic orbits.

A.1.3 Improving the initial condition

To identify an orbit with a unique starting point, an additional plane in phase space, the *Poincaré surface of section* $\mathcal{P}$, has to be defined. Starting with a random initial condition on $\mathcal{P}$, the trajectory and the reduced matrizant can be integrated as explained in the previous section. Having found another intersection with $\mathcal{P}$ close to the starting point, the reduced matrizant should be used to improve the initial condition.

For a simple notation, $\boldsymbol{\gamma}$ is the phase space vector (x, y, u, v) as given above, and the initial and final point are denoted by $\boldsymbol{\gamma}_i$ and $\boldsymbol{\gamma}_f$, respectively. The corresponding vectors in the local coordinate system are given by $\widehat{\boldsymbol{\gamma}}_i = \underline{U}^{-1}(0)\,\boldsymbol{\gamma}_i$ and $\widehat{\boldsymbol{\gamma}}_f = \underline{U}^{-1}(T)\,\boldsymbol{\gamma}_f$.[2] The second part of $\widehat{\boldsymbol{\gamma}} = (\widehat{\gamma}_1, \widehat{\gamma}_2, \widehat{\gamma}_3, \widehat{\gamma}_4)$, is denoted by $\widetilde{\boldsymbol{\gamma}} := (\widehat{\gamma}_3, \widehat{\gamma}_4)$. Starting at a distance $\delta\widetilde{\boldsymbol{\gamma}}$ to the initial point results, according to the definition of $\underline{\widetilde{\chi}}$ in Eq. (A.5), in a deviation $\Delta\widetilde{\boldsymbol{\gamma}} = \underline{\widetilde{\chi}}\,\delta\widetilde{\boldsymbol{\gamma}}$ from the final point. If the new starting point corresponds to a periodic orbit, i. e.

$$\begin{aligned} \widetilde{\boldsymbol{\gamma}}_i + \delta\widetilde{\boldsymbol{\gamma}} &\stackrel{!}{=} \widetilde{\boldsymbol{\gamma}}_f + \Delta\widetilde{\boldsymbol{\gamma}} \\ \Rightarrow \quad \delta\widetilde{\boldsymbol{\gamma}} &= (\mathbb{1} - \underline{\widetilde{\chi}})^{-1}\,(\widetilde{\boldsymbol{\gamma}}_f - \widetilde{\boldsymbol{\gamma}}_i)\,. \end{aligned} \tag{A.9}$$

All quantities on the r.h.s. of Eq. (A.9) are known explicitly, so that the necessary correction $\delta\widetilde{\boldsymbol{\gamma}} = (\widetilde{\gamma}_3, \widetilde{\gamma}_4)$ leading to a periodic can be calculated. Note that by the reduction to 2D no information is lost, since the two omitted basisvectors have eigenvalues 1. The correction $\delta\widetilde{\boldsymbol{\gamma}}$ can now be transformed back to the ordinary phase space coordinates via $\delta\boldsymbol{\gamma} = U(0)\,\delta\widehat{\boldsymbol{\gamma}}$, where $\delta\widehat{\boldsymbol{\gamma}} := (0, 0, \widetilde{\gamma}_3, \widetilde{\gamma}_4)$. This step introduces an additional error, since the local coordinate system of neither the initial point $U(0)$, nor of the final point $U(T)$ but of the *new* starting point gives the correct transformation. In practice, however, the difference is insignificant.[3] Apart from that small error, $\delta\widehat{\boldsymbol{\gamma}}$ is equivalent to the result of a calculation using the full 4D matrizant.

Taking $\boldsymbol{\gamma} = \boldsymbol{\gamma}_i + \delta\boldsymbol{\gamma}$ as the new starting point unfortunately

1. leaves the Poincaré surface of section.
   This is associated with the fact that the periodic orbit may have another period as the reference orbit. The initial correction therefore has to be extrapolated onto the Poincaré surface according to $\delta\widehat{\boldsymbol{\gamma}} + \delta t \cdot \dot{\boldsymbol{\gamma}} \in \mathcal{P}$.

[2] Please note that for non-closed orbits the local coordinate system for initial and final point are different.

[3] The best approximation feasible at this stage is a linear interpolation between the local coordinate systems. This does not improve the convergence.

2. violates energy conservation.
   The matrizant describes the linearization of deviations from the reference orbit, and thus is only energy conserving to linear order. To prevent a shift of energy, the starting condition has to be projected back on the energy surface.[4]

Including these two projection procedures, $\boldsymbol{\gamma} = \boldsymbol{\gamma}_i + \delta\boldsymbol{\gamma}_{\text{projected}}$ gives an improved initial condition.

A.1.4 Converging to a periodic orbit

In the linear regime of a periodic orbit, the scheme of the preceding section converges in a single step. If the initial condition is outside the linear regime, the procedure has to be iterated. Usually a few iteration steps (< 10) are sufficient to determine the initial condition within machine accuracy (i. e. $\approx 10^{-13}$). In closed systems nearly all starting conditions converge to a periodic orbit, so that periodic orbits are easily found. For open systems the trajectories have a finite probability to leave the system. This leads to an increased numerical effort, since several starts are needed to converge to a periodic orbit. For the channel the probability for a trajectory to leave the central antidot regime is so large that only a small fraction of initial conditions converges.

To converge to those unstable fixpoints whose incoming and outgoing manifold intersect on the Poincaré surface of section at an extremely small angle, it is sometimes useful to add only a fraction $0 < \kappa < 1$ of the calculated correction to the initial condition, i. e. $\boldsymbol{\gamma} = \boldsymbol{\gamma}_i + \kappa\delta\boldsymbol{\gamma}_{\text{projected}}$. This enlarges the radius of convergence for these special fixpoints, but also increases the number of iterations required.

Starting the above procedure with random points does not assure to find all periodic orbits in the system. The most relevant, however, are those with large amplitudes. These have a large radius of convergence, so that the probability of missing an important orbit is small. It can be further reduced by following the orbits through parameter space. Thereby one can conveniently check that no orbit is missed at a bifurcation. Furthermore, orbits can frequently be classified. For the channel system, the number of reflections in the constrictions together with the symmetry of the orbit gives such a classification. Missing orbits can readily be identified in such a scheme. All this establishes no proof, but combining these three methods can assure beyond reasonable doubt that the relevant orbits have been included.

A.2 Properties of the orbits

Once the above algorithm has converged, the properties of the newly determined periodic orbit have to be calculated. For the application of the trace formula the action S, the determinant of the monodromy matrix M, the period T_0, the Maslov index μ and the velocity-velocity correlation functions $\mathcal{C}_{ij}$ have to be evaluated. In systems with discrete symmetries, also the symmetry-related degeneracies have to be known.

[4] In practical applications it is often unnecessary to calculate the normal vector of the energy surface. It is generally sufficient to include the correction to the (absolutely) smaller component of the momentum (δu or δv) directly, and to determine the second momentum component from energy conservation. This simplification has hardly any influence on the convergence properties.

A.2.1 Period, action, stability and degeneracy

The period T_0 is automatically calculated when integrating the equations of motion. The action can be integrated straight-forward using

$$S = \int_0^{T_0} \boldsymbol{p}\, d\boldsymbol{q} = \int_0^{T_0} \boldsymbol{p}\dot{\boldsymbol{q}}\, dt\,, \tag{A.10}$$

with $\boldsymbol{p} = (x, y)$ and $\boldsymbol{q} = (u, v)$.

The stability of an orbit enters the trace formula via $\mathrm{Det}(\mathrm{M} - \mathbb{1})$. The monodromy matrix M is identical to the matrizant after one period, i. e. $M = \underline{\chi}(T_0)$. The determinant is neither affected by the unitary transformation $\underline{U}$, nor by the reduction to two dimensions, since the omitted eigenvalues are 1. Therefore

$$\mathrm{Det}(\underline{\chi} - 1) \;=\; \mathrm{Det}(\widehat{\underline{\chi}} - 1) \;=\; \mathrm{Det}(\widetilde{\underline{\chi}} - 1) \;=\; 2 - \mathrm{Tr}(\widetilde{\underline{\chi}})\,, \tag{A.11}$$

so that $\mathrm{Det}(\mathrm{M} - \mathbb{1})$ can be identified with $2 - \mathrm{Tr}(\widetilde{M})$. The stability matrix $\widetilde{M}$ is given by the reduced matrizant $\widetilde{\underline{\chi}}$ at $T = T_0$. The latter is already known from the convergence procedure.

The symmetry of an orbit can be determined numerically by calculating the intersections with suitable Poincaré surfaces of section. These have to be chosen according to the possible symmetries of the orbits, i. e. the symmetries of the system. Close to a bifurcation, however, the asymmetry of an orbit can be infinitesimal small, and thus covered by the numerical inaccuracies. Due to these limitations, the degeneracy cannot be determined numerically in the vicinity of a bifurcation. The degeneracy and the Maslov index of an orbit change only at bifurcation points. Following the orbits through parameter space (see appendix A.3), these quantities can conveniently be calculated sufficiently far from a bifurcation.

The channel considered in this work exhibits three discrete symmetries: with respect to reflection at the x-axis, the y-axis and the combination of these reflections, i. e. a rotation by π. A convenient Poincaré surface is given by $y = 0$. The orbits have anyway to be calculated for varying B and s_d in order to compare with the experimental findings. Therefore choosing B and s_d to be far from bifurcations does not lead to additional numerical effort.

A.2.2 Velocity-velocity correlation function

A nice idea[5] to reduce the numerical effort calculating $\mathcal{C}_{ij}$ is to express the velocity of the periodic orbit as a Fourier sum

$$v_i(t) = \bar{v}_i + \sum_{n=1}^{\infty} \left[a_{i,n}\, \sin(nwt) \;+\; b_{i,n}\, \cos(nwt)\right]\,, \tag{A.12}$$

where $w = 2\pi/T_0$, T_0 is the period of the orbit, and i stands for either x or y. Inserting this expression in Eq. (5.7), all integrations can be performed analytically. The final result reads

$$\mathcal{C}_{ij} = \frac{T_0}{2} \sum_{n=1}^{\infty} \frac{(a_{i,n}\, a_{j,n} + b_{i,n}\, b_{j,n})/\tau_s - (a_{i,n}\, b_{j,n} - a_{j,n}\, b_{i,n})nw}{(1/\tau_s)^2 + (nw)^2}\,. \tag{A.13}$$

[5] This idea of U. Rößler was communicated by R. Onderka.

The coefficients a_n and b_n can be calculated from the integrals

$$\begin{aligned} a_{i,n} &= \frac{2}{T_0}\int_0^{T_0} v_i(t)\sin(nwt)\,dt \quad \text{and} \\ b_{i,n} &= \frac{2}{T_0}\int_0^{T_0} v_i(t)\cos(nwt)\,dt\,. \end{aligned} \tag{A.14}$$

These integrations can again be performed simultaneously with the integration of the EOM.

A convenient method to check the convergence of the Fourier sum Eq. (A.12) is given by Parseval's theorem. For this special case it reads

$$\int_0^{T_0} |v_i(t)|^2 \;=\; \frac{2}{T}\sum_{n=1}^{\infty}\left[(a_{i,n})^2 + (b_{i,n})^2\right]\;. \tag{A.15}$$

In a numerical integration, where Eq. (A.12) has to be truncated, this relation allows a numerical calculation of the truncation error.

In the case of the channel system, all orbits are similar to cyclotron orbits. This leads to rapidly decaying higher harmonics. Furthermore, the first term in Eq. (A.13) can be neglected for those trajectories. This simplifies the calculation of $\mathcal{C}_{ij}$ to

$$\begin{aligned} \mathcal{C}_{xx} &\approx \frac{T_0\tau_s}{2}\sum_{n=1}^{\infty}\frac{(a_{x,n})^2 + (b_{x,n})^2}{1+(nw\tau_s)^2} \quad \text{and} \\ \mathcal{C}_{xy} &\approx \frac{T_0\tau_s}{2}\sum_{n=1}^{\infty}\frac{a_{y,n}\,b_{x,n} \;+\; a_{x,n}\,b_{y,n}}{1+(nw\tau_s)^2}\;nw\tau_s\,. \end{aligned} \tag{A.16}$$

For $w\tau_s > 1$, the higher Fourier components are additionally damped by the factor $1/(nw\tau_s)$. This is fulfilled for the channel with antidots considered in chapter 7. Therefore the inclusion of the leading 5 Fourier components was sufficient.

Note that the calculation of N Fourier components leads to $4N$ additional differential equations which have to be solved simultaneously to the EOM. It is therefore indicated to calculate only $\boldsymbol{\gamma}$ and $\widetilde{M}$ while converging to a periodic orbit, and to integrate the complete system of differential equations (including the action, the stability angle and the Fourier components) only once for each (converged) orbit.

A.2.3 Maslov index

The Maslov index is a geometrical winding number [22, 66]. This property will be used in the following for its numerical evaluation. The procedure presented here is similar to the one of Eckhardt and Wintgen [25], but it is numerically more convenient. It is much easier to implement than the general method presented by Creagh and Robbins [22, 66].[6] It is, however, restricted to two dimensional systems.

[6] Their approach is presented in a version accessible to numerical calculations in Ref. [100].

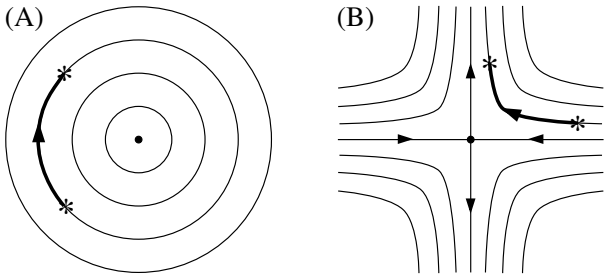

Figure A.1: *Local phase space portraits around a periodic orbit. (A) Stable, (B) unstable orbit.*

A periodic orbit is a fixpoint of the mapping of the Poincaré surface of section onto itself. The local linearization of the mapping is given by the reduced stability matrix[7]. Starting with a small deviation from the periodic orbit γ which corresponds to an eigenvector of $\widetilde{M}$, this deviation winds around γ. The total winding angle Θ is related to the Maslov index. This relation is different for the different types of fixpoints, i. e. periodic orbits. The local behavior around the fixpoint can easily be classified in dependence of the eigenvalues m_1, m_2 of the stability matrix $\widetilde{M}$:

stable orbits $\leftrightarrow |m_1| = |m_2| = 1$; Fig. A.1(A).
An orbit in the vicinity of a stable orbit remains on a ellipse around the fixpoint. All these ellipses map onto themselves. For stable orbits, the trace of the stability matrix is absolutely smaller than 2.

hyperbolically unstable orbits $\leftrightarrow m_1 = 1/m_2 > 1$; Fig. A.1(B).
Two lines in the Poincaré section map onto each other. Starting on one of these, the distance of the intersection points to the fixpoint exponentially grows ($m > 1$, outgoing manifold) or shrinks ($m < 1$, incoming manifold). Hyperbolically unstable orbits have $\mathrm{Tr}(\widetilde{M}) > 2$.

inverse hyperbolic orbits $\leftrightarrow m_1 = 1/m_2 < -1$
Equivalent to the hyperbolic case, but the intersection points change the side of the fixed point with each revolution. The trace of $\widetilde{M}$ of these orbits is smaller than -2.

For two dimensional unstable orbits the winding angle Θ is identical for all initial deviations, and a multiple of π (even multiple for the hyperbolic, and odd for the inverse hyperbolic case). This is obvious, since both the incoming manifold and the outgoing manifold map onto itself. The stability matrix is linear, so that this also holds for all linear combinations of these vectors, i. e. the whole surface of section.

For stable orbits, Θ is given by the winding angle of an eigenvector of $\widetilde{M}$. Now the winding angle is not a multiple of π, and it depends on the initial deviation. The common way to determine the winding angle is therefore to calculate first an eigenvector of $\widetilde{M}$, and to propagate this along the periodic orbit. This procedure can be simplified, so that a single integration yields Θ. This approach uses different informations about Θ, which are combined to uniquely define the winding angle.

The starting point is to write $\widetilde{M}$ as the product of a rotation and a positive definite symmetric matrix $\underline{T}$:

$$\widetilde{M} = \underline{T} \begin{pmatrix} \cos(\varphi) & \sin(\varphi) \\ -\sin(\varphi) & \cos(\varphi) \end{pmatrix} . \tag{A.17}$$

[7] Strictly speaking, the reduced (2D-) stability matrix is a mapping of the plane perpendicular to the orbit (at the initial point) and the energy surface onto itself. This distinction is, however, unimportant for the following discussion.

This is always possible, and the factorization is unique [95]. φ can easily be determined via

$$\varphi = \arctan\left(\frac{m_{12} - m_{21}}{m_{11} + m_{22}}\right) . \tag{A.18}$$

φ is a continuous function of t, and $\varphi|_{t=0} = 0$. To evaluate φ numerically, the stepsize of the differential equation solver has to be small enough so that subsequent φ differ by less than π. This condition is readily implemented in the adaptive stepsize control of the numerical integration. The correct branch $\varphi(t_n)$ can then be selected at every timestep with the knowledge of $\varphi(t_{n-1})$.

The integration of the EOM as described in Sec. A.1.4 calculates $\widetilde{\underline{\chi}}$ instead of $\widetilde{M}$. Since the local coordinate systems are identical at $t = 0$ and $t = T_0$, the winding angles in the local and the stationary system can only differ by integer multiples of 2π. The coordinate system Eq. (A.4) used above does not introduce those spurious windings [25]. Therefore, $\widetilde{\underline{\chi}}$ can be directly used to calculate φ.

Geometrically, φ describes the rotation of $\widetilde{M}$, and T a shearing. An arbitrary initial deviation is rotated by φ and sheared according to T. The shearing changes the direction of the vector by an angle α with $|\alpha| < \pi/2$. Furthermore, sign[tan(φ)]=sign[tan(Θ)]. The eigenvalues of $\widetilde{M}$ are given by $m_{1,2} = \exp(\pm i\Theta)$. This determines $|\Theta|$ modulo 2π. Combined, this information is sufficient to determine Θ uniquely. The description convenient for a numerical calculation reads

$$\begin{aligned} \Theta &= 2\pi \cdot \mathrm{INT}\left[\frac{\varphi+\pi}{2\pi}\right] + \widetilde{\Theta}\,\mathrm{sign}\left[\mathrm{mod}_2\left(\frac{\varphi+\pi}{2\pi}\right) - 1\right] , \quad \text{with} \\ \widetilde{\Theta} &= \left|\arctan\left(\frac{\sqrt{1 - \left(\mathrm{Tr}(\widetilde{M})/2\right)^2}}{\mathrm{Tr}(\widetilde{M})/2}\right)\right| . \end{aligned} \tag{A.19}$$

Here INT[x] stands for the largest integer smaller or equal to x, and mod_2 for the remainder in a division by 2.

The Maslov index is determined from the winding angle. For unstable orbits it is given by Θ in units of π

$$\mu = \Theta/\pi . \tag{A.20}$$

For stable orbits, μ is the nearest odd integer to the winding angle in units of π, i. e.

$$\mu = 1 + 2 \cdot \mathrm{NINT}\left[\frac{\Theta+\pi}{2\pi}\right] . \tag{A.21}$$

The winding angle scales with the repetition number of the orbit. The above formulas show, however, that the Maslov index only scales for unstable orbits with the repetition number. This makes the inclusion of higher repetitions of a stable orbit more complicated. Many authors therefore restrict themself to the generic case of completely chaotic systems, where all orbits are hyperbolically unstable. Having finally determined the Maslov index, all quantities needed for the evaluation of the semiclassical trace formula are known.

A.3 Following periodic orbits through parameter space

In order to calculate the semiclassical trace formula for different values of the external parameters (in the case of the channel system these are the magnetic field and the anti-dot diameter), it is desirable to have an algorithm which follows a specific orbit through parameter space. This can be achieved by iteratively changing marginally the parameter, followed by the convergence procedure described in Sec. A.1.4. This approach is frequently inapplicable, since (especially for very unstable orbits) the largest stepsize which still assures convergence is too small for any practical purpose. Extrapolating the initial conditions conditions to the new value of the parameter allows larger stepsizes. Note, however, that it is again necessary to ensure that the extrapolation remains on the surface of section and on the energy shell.
The choice of the extrapolation scheme is important for the performance of this approach. Linear interpolation is frequently not good enough, so that polynomial or rational function extrapolation is recommended. As pointed out in Ref. [104], extrapolations to too high orders tend to introduce spurious oscillations due to numerical inaccuracies of the data. In this work, rational function interpolation to 4th order was implemented. The starting condition in x and $\dot{x}$ was extrapolated to the new external parameter, y was fixed by the Poincaré surface of section, and $\dot{y}$ (the larger velocity component) was determined by energy conservation.

To reduce the computation time further, it is reasonable to introduce an adaptive stepsize control. The number of convergence steps needed can readily be used as a criterion for the next stepsize. The critical point is to ensure that, at the new value of the external parameter, the procedure does not converge to a different PO. For systems like the channel, where the initial conditions for many periodic orbits are close in phasespace, this requires special care. A convenient and reliable method is to check whether all orbit quantities vary smoothly. In this work, the following characteristic data of the orbits have been extrapolated to the new parameter value: Action S, stability $\mathrm{Tr}(\widetilde{M})$, period T_0 and winding angle Θ. The latter quantity is especially useful for systems with geometrically very similar orbits. The deviation of the extrapolation of these quantities to the orbit converged to was controlled, and too large deviations were rejected. In this case, a new extrapolation with reduced stepsize was started. It turned out that it is helpful to adapt the stepsize not only according to the number of iterations needed, but additionally to the extrapolated changes of the other orbit parameter. This applies especially in the vicinity of bifurcations.

This procedure works its way quickly through uninteresting terrain, slowing down where the starting conditions of the periodic orbits vary substantially. The storage requirements can be reduced by saving only those data points, where an *interpolation* of the neighboring points is worse than a tolerated error.

Furthermore it is convenient to include routines that can handle bifurcations. At the bifurcation the orbit is marginally stable, so that the convergence algorithm proposed above fails. This drawback can be overcome by first approaching the bifurcation point as close as possible. Then the initial conditions are extrapolated sufficiently far to the other side of the bifurcation, trying to converge to the orbit beyond the bifurcation. This procedure was implemented for period doubling bifurcations.